

# Strength and Deformation Characteristics of Electric Arc Furnace Slag as Ballast Aggregate

Meletetsega Gashaw<sup>1</sup>, Tadahiro Kishida<sup>1,2</sup>, George Mylonakis<sup>1,3</sup>

<sup>1</sup> Department of Civil & Environmental Engineering, Khalifa University, Abu Dhabi, UAE

<sup>2</sup>The Garrick Institute for the Risk Sciences, University of California, Los Angeles, CA 90095, USA

<sup>3</sup>School of Civil, Aerospace and Design Engineering (CADE), University of Bristol, Bristol, BS8 1QU, UK  
[100059794@ku.ac.ae](mailto:100059794@ku.ac.ae); [tadahiro.kishida@ku.ac.ae](mailto:tadahiro.kishida@ku.ac.ae); [george.mylonakis@ku.ac.ae](mailto:george.mylonakis@ku.ac.ae)

**Abstract** - The accumulation of waste by-products, such as steel slag, has become a significant environmental concern in waste management. In recent years, the reuse of waste materials in structural fills and pavement subbase materials has increased as part of efforts to promote sustainable waste recycling. On this basis evaluating potential alternative for railway ballast materials is valuable, particularly from the prospective of mechanical performance. This study examines the potential of EAF slag as a railway ballast material through a comprehensive series of laboratory tests, including physical and mechanical evaluations. Monotonic and cyclic triaxial tests are performed to evaluate its shear strength and permanent deformation characteristics under field representative stress condition. The performance of EAF slag is subsequently compared with various ballast materials reported in the literature. The results indicate that the EAF slag meets the standards established by major countries. Additionally, its performance aligns with previously published data for natural aggregate ballast materials, demonstrating promising shear strength, less permanent deformation, and improved stiffness under repeated loading.

**Keywords:** Railway ballast, EAF slag ballast, Drained triaxial test, Permanent deformation

## 1 Introduction

The ballast, a layer consisting of coarse aggregates surrounding the rail sleepers, provides essential support for stability, making it the most important component of the rail track substructure. Railway ballast materials are typically obtained from various types of rock, such as granite, basalt, rhyolite, quartzite and limestone, with volcanic rocks being the most common [1]. Based on local availability, economic considerations, and environmental regulations, it is critical to find suitable ballast materials [2]. Industrial wastes are often used in road embankments and land reclamation projects in areas where conventional fill materials are scarce (e.g., sand and gravel), and quarrying costs are excessively high [3]. Furthermore, the production of industrial waste materials, such as steel furnace slag from steel production, has been growing rapidly. Many researchers have investigated the application of steel slag on highways base and subbase layers, as well as in asphalt mixture aggregates [4]–[6], however, there is limited research evaluating EAF steel slag as a potential ballast material under working stress and various loading conditions. This study evaluates the performance of EAF slag, focusing on its physical and mechanical properties, including gradation, particle shape, specific gravity, dry and wet abrasion resistance, impact value, and water absorption. It also examines its strength and deformation characteristics, such as peak friction angle, permanent deformation, cyclic compression, and resilient modulus, using drained triaxial monotonic and cyclic compression tests. Finally, the applicability of EAF slag as a potential ballast material is discussed based on the results, with comparisons made to various natural aggregates reported in the literature.

## 2 Laboratory Test Program

### 2.1 Test Material

EAF slag, a by-product generated from the steel production industry using scrap metal, possesses a distinctive vesicular texture. It is notable for its high calcium, iron, and silica content, which contribute to its increased density and abrasion resistance, as highlighted in previous studies[7]. According to the sphericity-roundness evaluation framework by [8], the EAF steel slag aggregates have subangular form as shown in Figure 1a. Table 1 presents some key physical properties of the EAF slag aggregate used in the study. Table 2 presents some of the index properties of EAF slag compared to the ballast

specifications in USA and UK. It is seen that the index parameters are within the specification ranges for ballast aggregates according to the USA and UK specification. In addition, index parameters obtained for EAF slag are compared with natural aggregates in the literature. It is seen that EAF slag exhibits higher specific gravity, Los Angeles Abrasion (LAA), and Micro-Deval (MD) values compared to natural aggregate. The increased specific gravity of EAF slag is expected to enhance lateral track resistance [9], while its superior performance in LAA and MD tests suggests reduced degradation and crushing of ballast during track operation [10].

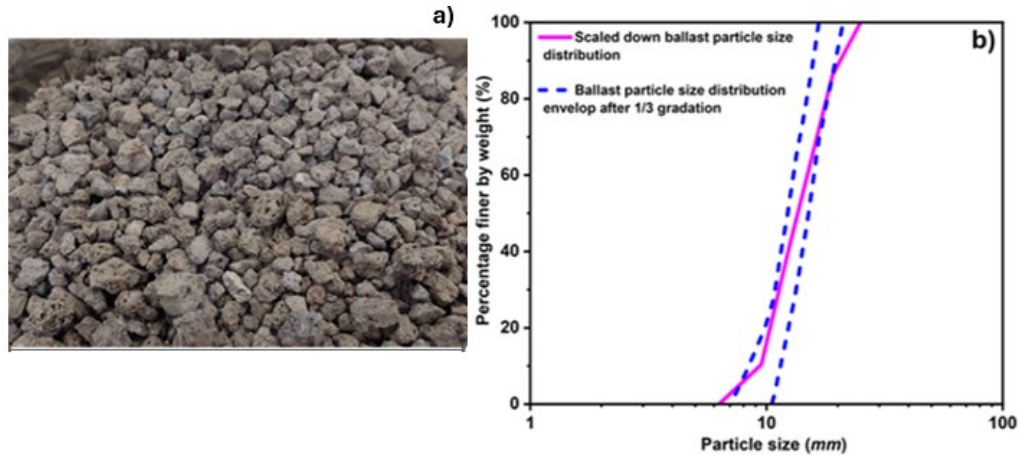


Figure 1 a) Picture of EAF slag used b) Particle size distribution curve of EAF slag after 1/3 parallel gradation

Table 1 Physical characteristics of materials used in the test

Properties	$d_{max}$ (mm)	$d_{min}$ (mm)	$C_u$	$e_{max}$	$e_{min}$	$G_s$	Particle shape
EAF Slag	19	6.3	1.6	0.931	0.654	3.44	Sub-angular

Table 2 Index parameters of EAF slag from USA and UK specification compared to other natural aggregates

Index parameter	Ballast specification		EAF Slag	Limestone [10]	Basalt [11]	Granite [12]
	USA[13]	UK[14]				
Specific gravity, $G_s$	$\geq 2.6$	-	3.44	2.63	2.81	2.7
Los Angeles Abrasion index (%)	$< 40$	$< 24$	14.6	25	9.94	15
Aggregate Impact value (%)	-	-	9.1	-	-	-
Micro-Deval index (%)	-	$\leq 5 - 15\%$	9.7	12.4	-	13
Water absorption	$\leq 2\%$	-	0.34	0.7	0.6	0.5

## 2.2 Triaxial Experiment Set Up

Figure 1b shows the particle gradation curve following a specific particle size distribution in line with UK ballast grading specifications [15]. Due to the triaxial apparatus's capacity, which accommodates samples up to 100 mm wide, a reduced particle size was used [7], ensuring a maximum particle-to-specimen diameter ratio between 5 and 6 [16]. Triaxial tests were carried out using a GCTS Testing System. The specimens, measuring 200 mm in height, were constructed under a vacuum of 20 kPa and enclosed in a rubber membrane with a 0.6 mm thickness. All samples were

prepared to a relative density ( $D_r$ ) of 70%. Specimens were saturated under back pressure, achieving a B-value greater than 0.95, and then isotopically consolidated under confining pressures of 30, 80, 120, and 200 kPa, before shearing commenced. A fully drained compression test was conducted at an axial strain rate of 1% per minute to allow complete dissipation of excess pore pressure. The shearing process was carried out until an axial strain of 10% was achieved. According to [17], a standard train with a 25-tonne axle load generates cyclic deviatoric stress of 230 kPa under confining stresses of 15-65 kPa. Recent studies on USA freight trains by [18] reported confining pressures up to 72 kPa under cyclic deviatoric stresses of up to 360 kPa. Therefore, this study selected cyclic deviatoric stresses of 230 and 350 kPa, corresponding to 25 and 40 tone axle loads with a confining pressure of 60, 80 and 120 kPa. The stress controlled cyclic tests with harmonic sinusoidal cyclic stress is performed in two phases. In the first stage a reduced frequency of conditioning phase was conducted for 100 cycles with a frequency of 0.1 Hz [3]. After that a frequency of 5 Hz was applied for next 20,000 cycles as the second and main loading phase.

### 3 Result and Discussion

#### 3.1 Monotonic Triaxial Test Results

A set of four isotopically consolidated drained triaxial compression tests were performed on EAF steel slag under effective confining stresses of 30, 80, 120, and 200 kPa. Figures 2a illustrate how the deviatoric stress varies with shear strain at different confining stress level. As expected, the deviatoric stress rises with increasing axial strain until a peak is reached. This peak deviatoric stress grows as the confining stress is increased from 30 to 200 kPa. However, defining peak strength was challenging due to the constant fluctuations in deviatoric stress caused by "stick-slip" processes with the large angular particles. Consequently, a distinct failure plane was not observed in these tests at 10% axial strain. Figures 2b illustrate the volumetric strain ( $\epsilon_v$ ) versus shear strain ( $\epsilon_q$ ) at different confining stress level. It shows that the  $\epsilon_v$  was initially compressive and became dilative as the  $\epsilon_q$  increased. The  $\epsilon_v$  shows a dilative to a compressive behavior as the confining pressure increased from 30 to 200 kPa.

Figure 3a shows the peak strength envelop of EAF steel slag. The averaged maximum stress ratio under compression loading was found to be 1.9, while its value tends to decrease as mean effective stress ( $p'$ ) at failure increases. Figure 3(b) shows the variation of peak friction angle ( $\phi_{peak}$ ) of EAF steel slag and other different ballast aggregates from literature tested under similar stress conditions [19], [12]. The  $\phi_{peak}$  reduces with increase in  $p'$ . In addition, the  $\phi_{peak}$  of EAF slag falls within the range of different ballast aggregates, indicating its comparable strength as potential ballast aggregate.

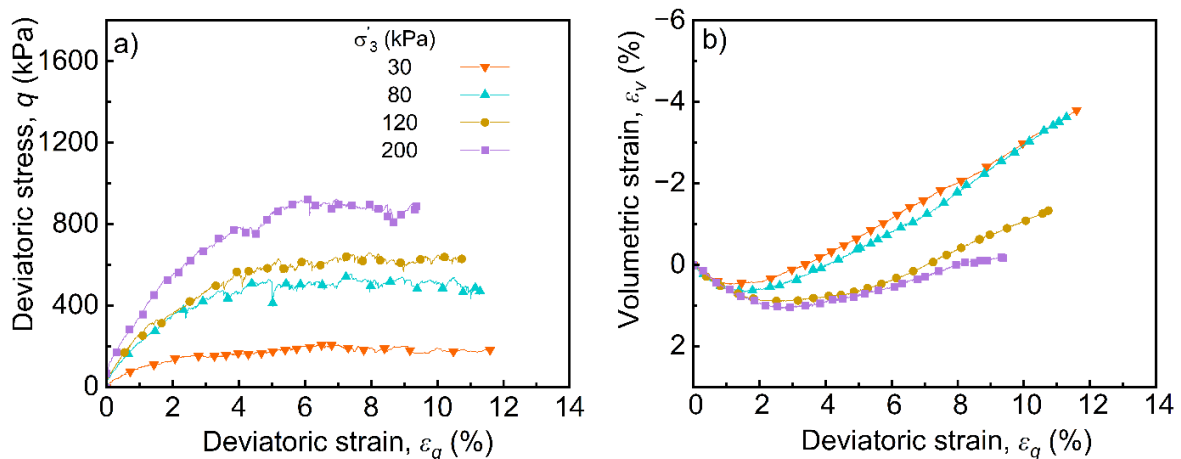


Figure 2 a) Deviatoric stress vs. deviatoric strain; b) volumetric strain vs. deviatoric strain from drained monotonic compression tests on EAF slag aggregates

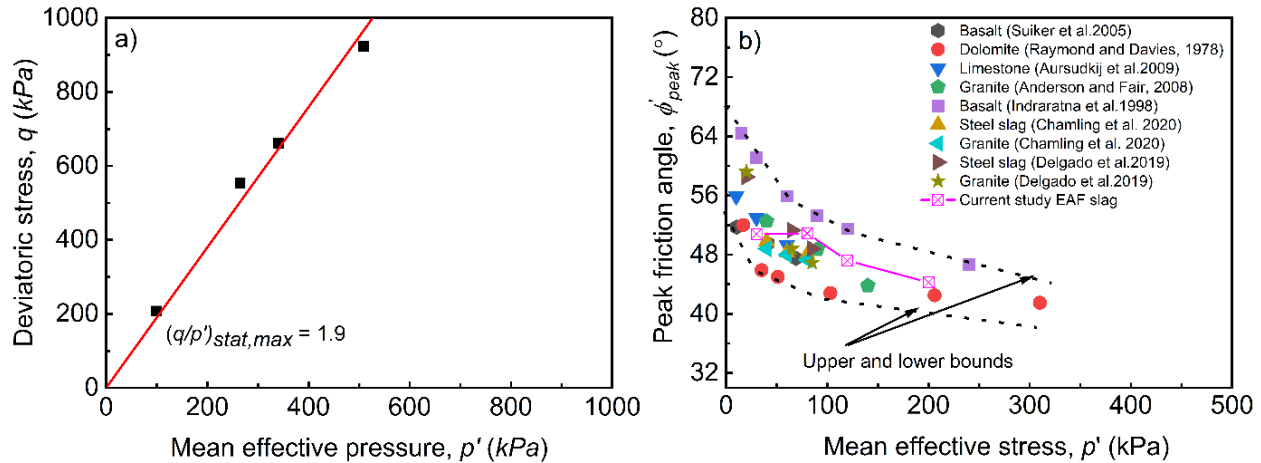


Figure 3 a) Peak strength envelop of EAF slag b) Variation of peak friction angle with mean effective stress at failure for EAF slag and various ballast materials

### 3.2 Cyclic Triaxial Tests Results

Figures 4(a) and 4(b) show the variations in permanent axial strains of EAF slag with the number of load cycles for applied cyclic loads of 230 and 350 kPa, respectively. It is seen that the permanent axial strain increases with the number of load cycles for both cyclic stresses, but rate of accumulation reduces as the number of cycles increases. The permanent axial deformation decreases with increase in confinement because the aggregates become stiffer and resistant for axial deformation as applied confining stress increases (Figure 4a and 4b). Moreover, the permanent axial deformation increases with increase in the amplitude of applied vertical stress from Figure 4a to 4b. This results are consistent with the previous studies [20]–[23]. Similarly, Figures 4(c) and (d) illustrate the variations of permanent volumetric strain with the number of cycles for 230 and 350 kPa, respectively. At lower cyclic stress amplitudes, increasing the confining pressure from 60 to 80 kPa slightly increased volumetric compaction, while increasing it to 120 kPa decreases volumetric compaction. In contrast, at higher cyclic stress ( $q_{max,cyc} = 350$  kPa), lower confining pressure induced greater volumetric strain due to sufficient energy for significant particle rearrangement. Higher confining pressures restricted lateral expansion and particle rearrangement, reducing volumetric deformation under high cyclic stress [24], [25]. Overall, volumetric strain significantly increased with higher applied cyclic loads.

Figure 5 presents the variation of the resilient modulus,  $M_r$  with number of load cycles. The resilient modulus is calculated as  $M_r = q_{max,cyc} / \epsilon_{a,rec}$ , where  $\epsilon_{a,rec}$  is the resilient axial strain during triaxial unloading. The resilient modulus ( $M_r$ ) increases with confining pressure due to enhanced particle stabilization, which reduces deformation and improves stiffness. Conversely,  $M_r$  decreases with higher cyclic stress amplitudes (350 kPa) as greater strain reduces stiffness. Additionally,  $M_r$  stabilizes after a certain number of loading cycles, similar to permanent strain behavior.

Figure 6 demonstrates the variation of permanent strains after 10,000 cycles for different natural aggregates from the literatures[20]–[23] compared to EAF slag in this study. Both final  $\epsilon_a$  and  $\epsilon_v$  of EAF slag are lower than the natural ballast aggregates indicating the better performance of EAF slag in resisting deformation under sustained cyclic loading. This may be attributed to its higher stiffness and rough structure, which enhanced interlocking. Reduced permanent vertical and volumetric strain offers advantages such as a thinner ballast layer and decreased maintenance demands [3], making EAF slag a more cost-effective option with an extended lifespan compared to natural aggregates. It is noted that various factors could affect the observed variations in final  $\epsilon_a$  at 10,000 cycles, including applied cyclic stress, confining pressure, initial density, frequency of cyclic stress and their combinations [20], [25], [26].

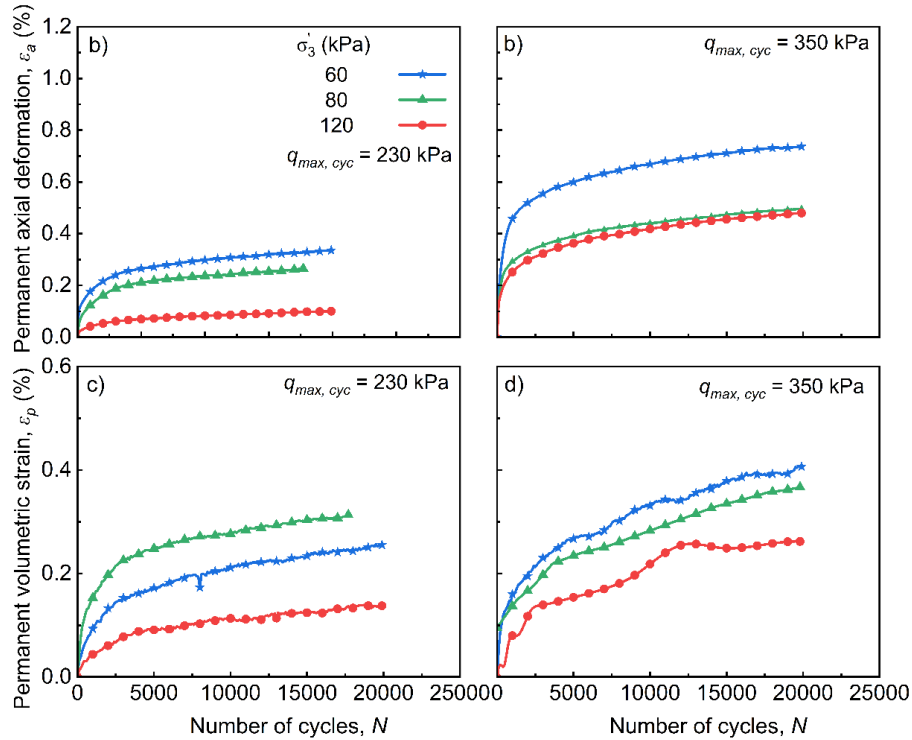


Figure 4 Variation of permanent axial strain with number of load cycles a) 230 kPa b) 350 kPa; Variation of permanent volumetric strain with number of load cycles c) 230 kPa d) 350 kPa.

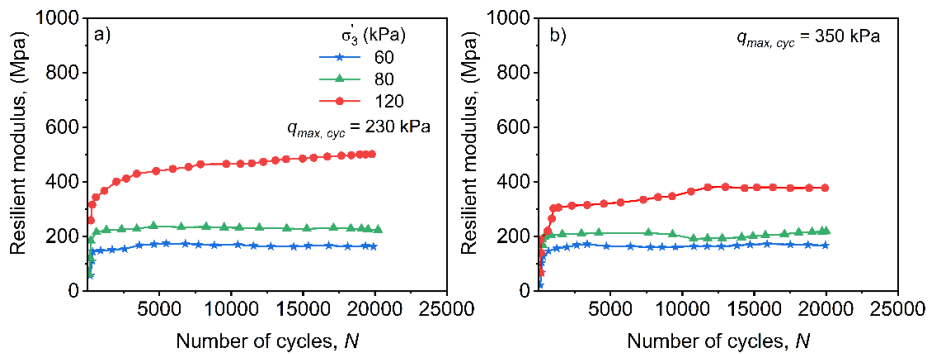


Figure 5 Variation of resilient modulus with number of load cycles

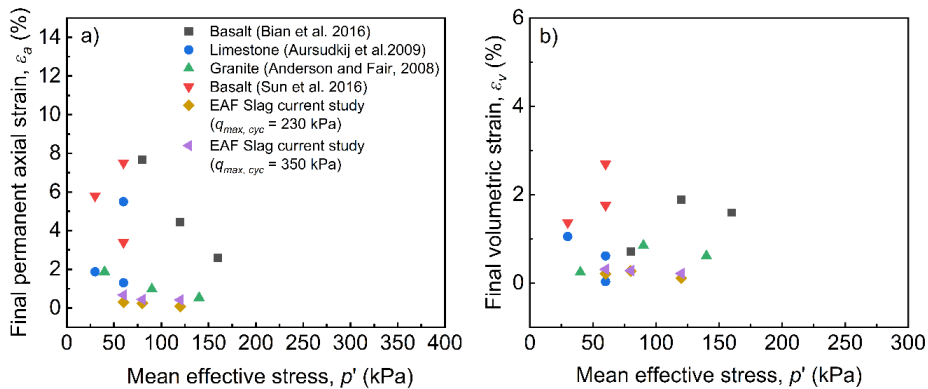


Figure 6 Comparison of final strains after 10,000 cycles a) permanent axial strain vs confining pressure b) permanent volumetric strain vs confining pressure

## 4 Conclusion

The behavior of EAF steel slag was assessed in the laboratory by conducting a series of physical, mechanical, and CID triaxial compression and cyclic loading tests, utilizing the parallel gradation technique. Additionally, the experimental results from various ballast materials are collected from multiple regions to compare with EAF slag performance. The results of physical tests show that EAF slag satisfy the gradation and shape requirements for railway ballast, and that it exhibits higher specific gravity and density. The results of mechanical tests show that EAF slag exhibits strong resistance to abrasion, impact, and crushing, making it highly suitable for use as ballast material. In addition, its mechanical properties were within the recommended values for railway ballast from UK and USA specifications. CID triaxial compression tests reveal that the peak strength of EAF slag is comparable to the strength of majority of natural ballast aggregates from the literatures and it decrease with increase in applied confining pressure. The cyclic triaxial tests show that the permanent deformation and resilient modulus of EAF slag depends on the applied confining pressure and magnitude of applied cyclic stress. Permanent strain reduces as confining pressure increase due to the additional lateral resistance while it increases with applied cyclic stress. However, comparison from previous literature the final permanent axial and volumetric strains after 10,000 cycles were significantly lower than the natural aggregates. This indicates the better performance of EAF slag as ballast aggregate by providing better resistance to deformation for long term cyclic loads.

## References

- [1] S. Aingaran, "Experimental investigation of static and cyclic behaviour of scaled railway ballast and the effect of stress reversal," 2014.
- [2] B. Indraratna and W. Salim, *Mechanics of Ballasted Rail Tracks: A Geotechnical Perspective*. CRC Press, 2005.
- [3] P. K. Chamling, S. Haldar, and S. Patra, "Physico-Chemical and Mechanical Characterization of Steel Slag as Railway Ballast," *Indian Geotech. J.*, vol. 50, no. 2, pp. 267–275, 2020, doi: 10.1007/s40098-020-00421-7.
- [4] A. E. A. E. M. Behiry, "Evaluation of steel slag and crushed limestone mixtures as subbase material in flexible pavement," *Ain Shams Eng. J.*, vol. 4, no. 1, pp. 43–53, 2013, doi: 10.1016/j.asej.2012.07.006.
- [5] S. Jahangirnejad, T. Van Dam, D. Morian, K. Smith, R. Perera, and S. Tyson, "Blast furnace slag as sustainable material in concrete pavements," *Transp. Res. Rec.*, no. 2335, pp. 13–19, 2013, doi: 10.3141/2335-02.
- [6] S. Mathur, S. K. Soni, and A. Murty, "Utilization of industrial wastes in low-volume roads," *Transp. Res. Rec.*, no. 1652, pp. 246–256, 1998.
- [7] B. G. Delgado, A. Viana da Fonseca, E. Fortunato, A. Paixão, and R. Alves, "Geomechanical assessment of an inert steel slag aggregate as an alternative ballast material for heavy haul rail tracks," *Constr. Build. Mater.*, vol. 279, 2021, doi: 10.1016/j.conbuildmat.2021.122438.
- [8] W. C. Krumbein and L. L. Sloss, *Stratigraphy and sedimentation*, Second Edi. San Francisco: W.H. Freeman and Company, 1963.
- [9] A. Hussain and S. K. K. Hussaini, "Use of steel slag as railway ballast: A review," *Transp. Geotech.*, vol. 35, no. April, p. 100779, 2022, doi: 10.1016/j.trgeo.2022.100779.
- [10] M. Esmaeili, R. Nouri, and K. Yousefian, "Experimental comparison of the lateral resistance of tracks with steel slag ballast and limestone ballast materials," *Proc. Inst. Mech. Eng. Part F J. Rail Rapid Transit*, vol. 231, no. 2, pp. 175–184, 2017, doi: 10.1177/0954409715623577.
- [11] G. Jing, J. Wang, H. Wang, and M. Siahkouhi, "Numerical investigation of the behavior of stone ballast mixed by steel slag in ballasted railway track," *Constr. Build. Mater.*, vol. 262, p. 120015, 2020, doi: 10.1016/j.conbuildmat.2020.120015.
- [12] B. G. Delgado, A. Viana da Fonseca, E. Fortunato, and P. Maia, "Mechanical behavior of inert steel slag ballast for heavy haul rail track: Laboratory evaluation," *Transp. Geotech.*, vol. 20, no. April, p. 100243, 2019, doi: 10.1016/j.trgeo.2019.100243.
- [13] AREMA (American Railway Engineering Maintenance-of-way Association), "Manual for Railway Engineering, Vol. I–IV.," Lanham, USA, 2015.
- [14] 13450 EN, "European Committee for Standardization. Aggregates for Railway Ballast," Brussels, 2002.
- [15] Railtrack Line Specification, "RT/CE/S/006 Issue 3. Track Ballast," 2000.
- [16] B. Indraratna, D. Ionescu, and H. D. Christie, "Shear Behavior of Railway Ballast Based on Large-Scale Triaxial Tests,"

- J. Geotech. Geoenvironmental Eng.*, vol. 124, no. 5, pp. 439–449, 1998, doi: 10.1061/(asce)1090-0241(1998)124:5(439).
- [17] B. Indraratna, C. Rujikiatkamjorn, and J. S. Vinod, “A review of ballast characteristics , geosynthetics , confining pressures and native vegetation in rail track stabilisation,” *Transp. Eng. Aust.*, vol. 12, no. 1, pp. 25–36, 2009.
- [18] T. D. Stark and R. H. Swan, “Railroad Ballast Testing and Properties,” *Railr. Ballast Test. Prop.*, 2018, doi: 10.1520/stp1605-eb.
- [19] A. S. J. Suiker, E. T. Selig, and R. Frenkel, “Static and Cyclic Triaxial Testing of Ballast and Subballast,” *J. Geotech. Geoenvironmental Eng.*, vol. 131, no. 6, pp. 771–782, Jun. 2005, doi: 10.1061/(ASCE)1090-0241(2005)131:6(771).
- [20] Q. D. Sun, B. Indraratna, and S. Nimbalkar, “Deformation and Degradation Mechanisms of Railway Ballast under High Frequency Cyclic Loading,” *J. Geotech. Geoenvironmental Eng.*, vol. 142, no. 1, pp. 1–12, 2016, doi: 10.1061/(asce)gt.1943-5606.0001375.
- [21] W. F. Anderson and P. Fair, “Behavior of Railroad Ballast under Monotonic and Cyclic Loading,” *J. Geotech. Geoenvironmental Eng.*, vol. 134, no. 3, pp. 316–327, 2008, doi: 10.1061/(asce)1090-0241(2008)134:3(316).
- [22] B. Aursudkij, G. R. McDowell, and A. C. Collop, “Cyclic loading of railway ballast under triaxial conditions and in a railway test facility,” *Granul. Matter*, vol. 11, no. 6, pp. 391–401, 2009, doi: 10.1007/s10035-009-0144-4.
- [23] X. Bian, J. Jiang, W. Jin, D. Sun, W. Li, and X. Li, “Cyclic and Postcyclic Triaxial Testing of Ballast and Subballast,” *J. Mater. Civ. Eng.*, vol. 28, no. 7, p. 04016032, 2016, doi: 10.1061/(asce)mt.1943-5533.0001523.
- [24] C. Gu, Y. Zhan, J. Wang, Y. Cai, Z. Cao, and Q. Zhang, “Resilient and permanent deformation of unsaturated unbound granular materials under cyclic loading by the large-scale triaxial tests,” *Acta Geotech.*, vol. 15, no. 12, pp. 3343–3356, 2020, doi: 10.1007/s11440-020-00966-0.
- [25] Q. Sun, Q. Dong, Y. Cai, and J. Wang, “Modeling permanent strains of granular soil under cyclic loading with variable confining pressure,” *Acta Geotech.*, vol. 15, no. 6, pp. 1409–1421, 2020, doi: 10.1007/s11440-019-00868-w.
- [26] J. Lackenby, B. Indraratna, G. McDowell, and D. Christie, “Effect of confining pressure on ballast degradation and deformation under cyclic triaxial loading,” *Geotechnique*, vol. 57, no. 6, pp. 527–536, 2007, doi: 10.1680/geot.2007.57.6.527.